Three-Dimensional Quantification of Nanoparticles by Electron Tomography –Improvement of Binarization Parameters

J. Leschner, A. Chuvilin, J. Biskupek, and U. Kaiser

Ulm University, Central Facility of Electron Microscopy, Electron Microscopy Group of Materials Science, 89081 Ulm, Germany

jens.leschner@uni-ulm.de
Keywords: electron tomography, quantification, binarization

Electron tomography is used to study in detail objects in the micro- to nanometer regime. Whereas the technique is used in biology to solve mostly topological questions, in material science the intensity produced by Z-contrast [1] is used in addition to distinguish different types and quantities of a material, e.g. for the case of embedded catalytic particles or embedded semiconductor nanoparticles. In order to quantify reliably their size and shape depending sensitively on the threshold, there is a strong demand for guidelines [2] in data-binarization.

Therefore, an extensive simulation study was performed with a number of parameters varied, in order to derive the necessary threshold. Due to artefacts, resulting either from the missing wedge problem, i.e. the elongation [3], or the reconstruction, i.e. anisotropic variation of the intensity [4], the simulation was carried out for the elongation-free acquisition-scheme of ±90°. Herewith, we concentrated on the impact of the reconstruction algorithm and solved the problem of unknown threshold [5]. We studied by spherical phantoms the impact of intensity (different material content) and of volumetric position (with respect to the tilt axis and to the z-height) on the chosen SIRT reconstruction from XMIPP [6] by identifying the threshold and comparing the ±90° to the ±75° (Fig. 1, 2) acquisition-scheme [7]. We show the limitations and improve our so far derived binarization-scheme.

We apply our derived knowledge on the $ErSi_2$ nanoparticles in 4H-SiC that was studied previously for their growth mechanism [8-10]. We exemplify our results by quantification of the particle volume with respect to the implantation depth of experimentally acquired data (±75° tilt-series of slab-like sample geometry and ±90° tilt-series of focused-ion-beam prepared needle-like sample geometry).

1. P.A. Midgley, M. Weyland, Ultramicroscopy 96 (2003), p. 413.
2. H. Friedrich, M. R. McCartney and P. R. Buseck, Ultramicroscopy 106 (2005), p. 18.
3. T. Kaneko, H. Nishioka, T. Nishi, H. Jinnai, J. of Electron Microscopy 54 (2005), p. 437.
4. S. Doré, R.E. Kearney, Medical & Biological Engineering & Computing 42 (2004), p. 591.
5. N. Kawase, M. Kato, H. Nishioka, H. Jinnai, Ultramicroscopy 107 (2007), p. 8.
6. C.O.S. Sorzano, R. Marabini, J. Velázquez-Muriel, et al., Journal of Structural Biology 148 (2004), p. 194.
7. J. Leschner, A. Chuvilin, J. Biskupek, and U. Kaiser, 3rd Int. Symp. On “Trends in Nanoscience 2009”, Monastery of Irsee, Germany; Abstract P-47.
8. U. Kaiser, D.A. Muller, J.L. Grazul, A. Chuvilin, M. Kawasaki, Nature Materials 1 (2002), p. 102.
9. C. Kübel, U. Kaiser, Microscopy and Microanalysis 12 (2006), p. 1546.
10. This work has been supported by the German Research Foundation (DFG) – project KA1295/7-1.

G. Kothleitner, M. Leisch (Eds.): MC2009, Vol. 1: Instrumentation and Methodology,
DOI: 10.3217/978-3-85125-062-6-043, © Verlag der TU Graz 2009

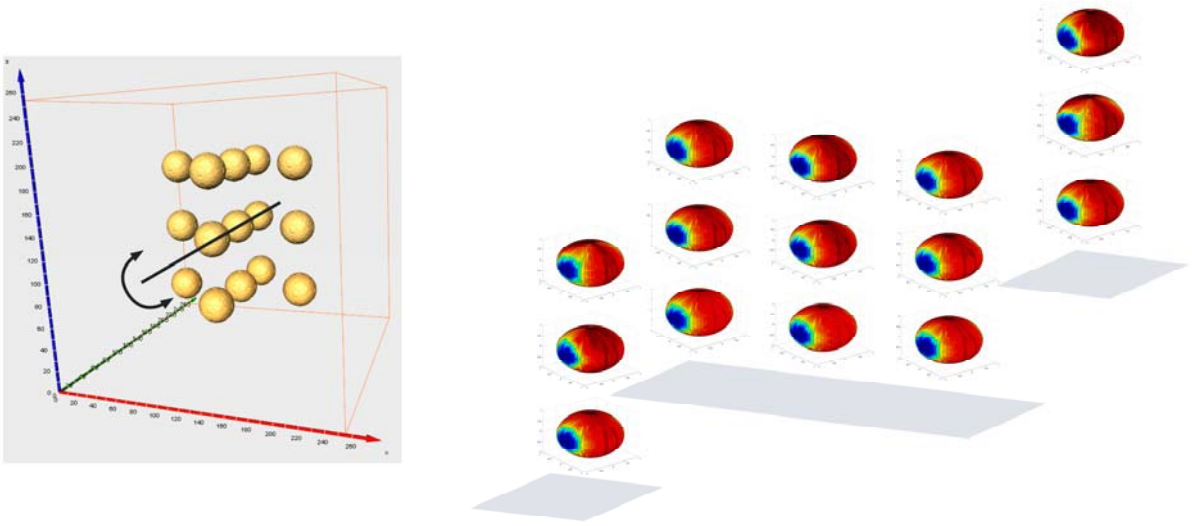

Figure 1. Threshold-maps for a missing-wedge-free acquisition-scheme of ±90°: (left) phantom of spheres distributed along and perpendicular to the tilt-axis represented by the black line; (right) threshold-maps for all spheres in the front, middle and back plane indicated by gray planes. A perfect reconstruction along the tilt-axis (blue: a threshold value of zero shows perfect reconstruction) and a non-perfect reconstruction perpendicular to it (red: indicating a threshold unequal to zero) are revealed. The fact that all spheres show similar shading reveals a constant binarization-scheme within the volume.

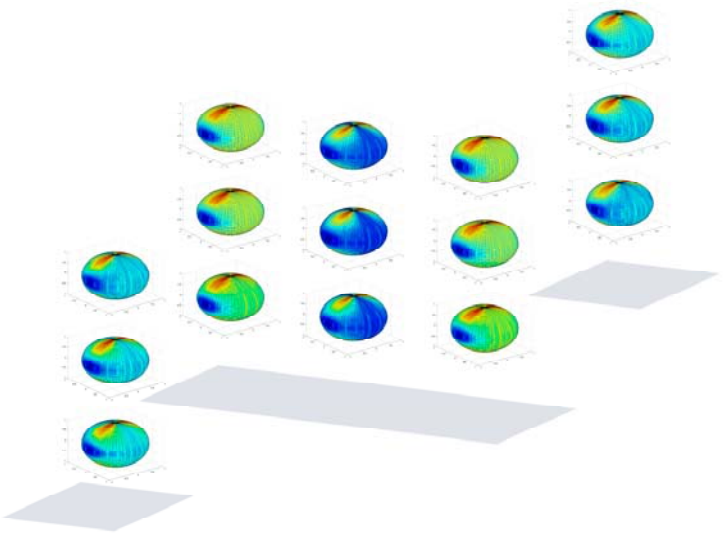

Figure 2. Identified threshold-maps of the phantom from Figure 1(left) for a limited tilt-range of ±75°. It reveals the missing-wedge artefact on top and at the bottom of each sphere in addition to the basic dependence as shown in Figure 1. In addition a position-dependence within the volume can be clearly seen as the shading differs from sphere to sphere.

G. Kothleitner, M. Leisch (Eds.): MC2009, Vol. 1: Instrumentation and Methodology,
DOI: 10.3217/978-3-85125-062-6-043, © Verlag der TU Graz 2009